BIOCHEMISTRY
including biophysical chemistry & molecular biology
Article

Biochemistry **2010,** *49,* 4327–4338 4327
DOI: 10.1021/bi901945w

Heme Binding to the Mammalian Circadian Clock Protein Period 2 Is Nonspecific[†]

Michael V. Airola,[‡] Jing Du,[§] John H. Dawson,[§] and Brian R. Crane*,[‡]

[‡]*Department of Chemistry and Chemical Biology, Cornell University, Ithaca, New York 14853, and* [§]*Department of Chemistry and Biochemistry, University of South Carolina, Columbia, South Carolina 29208*

Received November 11, 2009; Revised Manuscript Received March 2, 2010

ABSTRACT: The mammalian circadian clock synchronizes physical and metabolic activity with the diurnal cycle through a transcriptional−posttranslational feedback loop. An additional feedback mechanism regulating clock timing has been proposed to involve oscillation in heme availability. Period 2 (PER2), an integral component in the negative feedback loop that establishes circadian rhythms in mammals, has been identified as a heme-binding protein. However, the majority of evidence for heme binding is based upon *in vitro* heme-binding assays. We sought to ascertain if these largely spectral assays could distinguish between specific and nonspecific heme interactions. Heme-binding properties by a number of other well-characterized proteins, all with no known biological role involving heme interaction, corresponded to those displayed by PER2. Site-directed mutants of putative heme-binding residues identified by MCD were unable to locate a specific heme-binding site on PER2. Protein film electrochemistry also indicates that heme binds PER2 nonspecifically on the protein surface. Our results establish the inability of qualitative *in vitro* assays to easily distinguish between specific and nonspecific heme binding. We conclude that heme binding to PER2 is likely to be nonspecific and does not involve the hydrophobic pocket within the PER2 PAS domains that in other PAS proteins commonly recognizes cofactors. These findings also question the significance of *in vivo* studies that implicate heme interactions with the clock proteins PER2 and nPAS2 in biological function.

In mammals, physical and metabolic activity is synchronized with the diurnal cycle by the circadian clock (*1*−*4*). The clock acts as a gestalt, where the interactions of a few core clock gene products result in a remarkably precise molecular timepiece. The basic mechanism of the clock involves two transcriptional activators, CLOCK and bMAL1, whose activity oscillates over a 24 h cycle. Heterodimerization of CLOCK and bMAL1 initiates the transcription of various clock-controlled genes (CCGs) as well as two sets of core clock genes: period (*per1*, *per2*, and *per3*) and cryptochrome (*cry1* and *cry2*) (*1*−*4*). Time is set by a delayed transcriptional and posttranslational feedback loop dependent on the cellular location and levels of the Period (PER1 and PER2) and Cryptochrome (CRY1 and CRY2) proteins. After transcription of *per* and *cry* genes is initiated, their corresponding proteins begin to accumulate in the cytoplasm and eventually translocate into the nucleus where they inhibit transcriptional activity of the CLOCK/bMAL1 complex. Consequently, transcription of the *per* and *cry* genes halts, ultimately decreasing the levels of PER and CRY low enough to restore activity to the CLOCK/bMAL1 complex, thereby starting the cycle anew.

A large number of clock genes contain PAS domains that sustain the clock through protein−protein interactions (*1*, *4*, *5*). The PAS domain is a common protein fold present in every division of life. They often function as sensory modules that regulate the activity of an attached catalytic domain or an intermolecular partner. A variety of cofactors have been identified to bind inside the hydrophobic pocket of different PAS domains, which thereby enables a diverse set of signals to be sensed and relayed. For example, the bacterial protein FixL exploits a heme functional group to respond to oxygen depletion, modulating the activity of a downstream histidine kinase domain (*6*). Alternatively, the fungal photoreceptor vivid (VVD) utilizes an FAD molecule to synchronize metabolic activity to changing levels in blue light (*7*).

In addition to binding cofactors, some PAS domains participate primarily in protein−protein interactions. The PAS domains of the mammalian clock protein PER2 fall into this class with the recently determined crystal structure lacking any bound cofactors (*5*). Another member is the *Drosophila melanogaster* clock protein Period (dPER) which contains two PAS domains, both devoid of a cofactor. dPER's role in signal transduction appears to involve a change in dimerization between homodimerization and heterodimerization with the *Drosophila* Timeless clock protein (*5*, *8*). A further example is the aryl hydrocarbon receptor nuclear translocator (ARNT), a basic helix−loop−helix (bHLH)/PAS protein that forms heterodimeric transcriptional complexes with other bHLH/PAS proteins (*9*). ARNT complex formation with aryl hydrocarbon receptor (AhR) is mediated by ligand binding by AhR. However, complex formation of ARNT with hypoxia-inducible factor α (HIF-α) has analogy to clock protein interactions, being dependent on protein localization and degradation (*9*). It is unclear if these apo-PAS domains require cofactors for function *in vivo* (*10*, *11*), but their increasing representation within the PAS family suggests signaling mechanisms independent of any cofactor. In keeping with this, many PAS domains overexpressed in *Escherichia coli* do not purify with a bound cofactor (*5*, *8*, *11*, *12*).

Recent evidence has implicated that heme participates in a feedback loop that regulates the circadian clock. Heme addition is capable of synchronizing gene expression in NIH (3T3)

[†]This work was supported by NIH Grant GM079679 (B.R.C.), NIH Grant GM26730 (J.H.D.), and NIH Training Grant GM08267 (M.V.A.)

*To whom correspondence should be addressed. Telephone: (607) 255-8634. Fax: (607) 255-1248. E-mail: bc69@cornell.edu.

Published on Web 04/22/2010

cells (*13*). In turn, the clock controls transcription of δ-aminolevulinate synthase 1 (ALAS1), the rate-limiting enzyme for heme biosynthesis (*14*, *15*). Furthermore, core clock components have been identified as heme-binding proteins. Neuronal PAS domain protein 2 (nPAS2), a transcription factor homologous to CLOCK, has been shown to bind heme through its PAS domains and function as a gas-based sensor (*16*−*18*). PER2 has also been shown to bind heme through its PAS domains (*13*, *19*) and a downstream region of the protein that contains a putative novel heme-binding motif (*20*). Because of these interactions, heme has been suggested to modulate the activity of nPAS2 and the stability of PER2 (*19*, *20*). In addition, heme is the ligand for the nuclear steroid receptor REV-Erbα, a crucial element of the clock that regulates transcription of bMAL1 (*21*, *22*). Thus binding of heme to clock proteins could generate a feedback mechanism where the clock controls levels of heme through ALAS1 expression, and heme reciprocally regulates clock proteins by directly affecting their activity and stability.

To address the role of heme in the regulation of the circadian clock, we tested the hypothesis that the PAS domains of PER2 bind heme. In agreement with a previous study (*19*) we found that PER2 is capable of binding heme through its PAS domains. However, site-directed mutational analysis was unable to disrupt binding of heme to PER2 in any significant way. Heme is a hydrophobic molecule that is known to aggregate in aqueous solution and require detergents to maintain monodispersity (*23*, *24*). This led us to test if heme was binding to PER2 in a nonspecific manner due to hydrophobic and general ligand interactions. As a control, heme binding to well-characterized proteins, encompassing a breadth of functionalities, was assayed. None of these proteins utilize a heme moiety *in vivo*, but surprisingly all were found to bind heme *in vitro* in a manner comparative to PER2 and nPAS2. Our data suggest that the observed spectral changes reported for PER2 and nPAS2 are due to nonspecific binding of heme to hydrophobic patches and exposed ligands on the surface of these proteins.

MATERIALS AND METHODS

Cloning, Expression, and Purification. mPER2 DNA fragments encoding for amino acids 1−506, 1−320, and 972−1257 were PCR amplified and cloned into pET28 using *Nde*I or *Nhe*I and *Xho*I restriction sites. mPER2 mutants were generated using the QuikChange site-directed mutagenesis kit (Stratagene). All clones were confirmed by complete nucleotide sequencing. For overexpression of His-tagged PER2 proteins, plasmids were transformed into BL21(DE3) cells. An overnight culture was used to inoculate 2 L of Luria broth (LB). Cells were grown at 37 °C to an OD_{600} = 0.4, and then the temperature was reduced to 18 °C. After 1 h at 18 °C (OD_{600} = 0.8−1.0) protein expression was induced with addition of 100 μM IPTG. Cells were harvested by centrifugation 20 h after induction, and cell pellets were stored at −80 °C. All PER2 proteins were purified using standard metal affinity chromatography procedures. All protein buffers contained either 1−2 mM DTT or 0.5−1 mM TCEP to prevent disulfide formation. Overnight digestion with thrombin produced His-tag free protein as assessed by SDS−PAGE. To remove soluble aggregates, all proteins were further purified by size exclusion chromatography on a Superdex 200 26-60 Hi-Prep column. YqeH, CheA, and YtvA were purified as previously described (*25*−*27*). Incorporation of heme into purified protein was accomplished by incubation of a slight molar excess of hemin solution to PER2 proteins. The resulting solution was desalted on a Bio-Rad 10-DG desalting column to remove excess heme. The heme precursor, δ-levulinic acid, was also added to *E. coli* cells harboring the PER2 plasmid at the time of induction but did not result in any heme incorporation into PER2.

Cysteine Modification. A protein sample of PER2 129−506 (1 mM) was incubated with 3 mM TCEP for 1 h to ensure reduction of all cysteine residues. Reduced protein was incubated with 20 mM iodoacetamide for 30 min in Tris buffer, pH 8.0, and 150 mM NaCl. The reaction was quenched with a 5-fold excess of DTT. Protein was desalted and further purified by gel filtration.

UV−*Visible Absorption Spectroscopy*. Absorption spectra for mPER2 (1−506) and PAS A were recorded at 25 °C in stoppered quartz cuvettes with an Agilent 8453 UV−visible absorption spectrophotometer. Ferric samples were prepared in an anaerobic glovebox by diluting concentrated protein in previously degassed sample buffer. Subsequent treatment with dithionite produced the ferrous species.

Magnetic Circular Dichroism Spectroscopy. MCD spectra were measured with a magnetic field strength of 1.41 T by using a JASCO J815 spectropolarimeter. This instrument was equipped with a JASCO MCD-1B electromagnet and interfaced with a Silicon Solutions PC through a JASCO IF-815-2 interface unit. All spectral measurements for PAS A were carried out with a 0.2 cm quartz cuvette at 4 °C. Ferric samples were prepared by diluting concentrated protein into previously degassed sample buffer. Complete reduction of the heme iron was accomplished by adding a few microliters of concentrated sodium dithionite solution (25 mg/mL of H_2O) with a microliter syringe. Ferrous−CO adducts were prepared by bubbling CO gas into the ferrous PAS A samples. UV−visible absorption spectra were recorded with a Cary 400 spectrophotometer interfaced to a Dell PC before and after the MCD measurements to verify sample integrity.

Heme Titration Assay. Hemin-Cl (Sigma) was resuspended in 0.01 M NaOH, filtered using a 0.1 μm filter, and diluted with 100 mM Tris, pH 7.5, and 100 mM NaCl to generate a dilute heme solution. Purified protein was titrated stepwise into heme solution and thoroughly mixed. Spectra were recorded after each protein addition. The heme solution was pretreated with dithionite to generate ferrous heme. Titrations with ferrous heme were carried out with degassed solutions, under anaerobic conditions, in stoppered cuvettes. Direct calculation of binding constants was complicated by the presence of multiple heme-binding sites that varied depending on the protein studied. To determine a comparable value for binding affinity, we calculated heme absorption 50% (HA_{50}) values by taking the ratio of protein concentration to heme concentration at half the maximum absorbance change. All titrations were carried out with a similar heme concentration ranging from 3.2 to 4.5 μM, except for PER2 (1−506), where the titration employed 10 μM heme.

Heme Dissociation Kinetics. Hemin loss was measured using the H64Y/V68F apomyoglobin assay described by Hargove et al. (*28*). Purified proteins were preequilibrated with hemin in a 5 to 1 molar ratio. The reaction was measured as an increase in absorbance at 410 or 600 nm (for YtvA 600 nm was chosen because of the interfering absorption from the flavin cofactor at 410 nm) upon addition of a 6-fold molar excess of apomyoglobin H64Y/V68F to the protein of interest. Measurements were carried out with an Agilent 8453 UV−visible absorption spectrophotometer at 25 °C and in 0.2 M sodium phosphate, pH 7.0, and 0.45 M sucrose buffer. Rate constants were calculated by fitting the data to either single exponential and biexponential decay

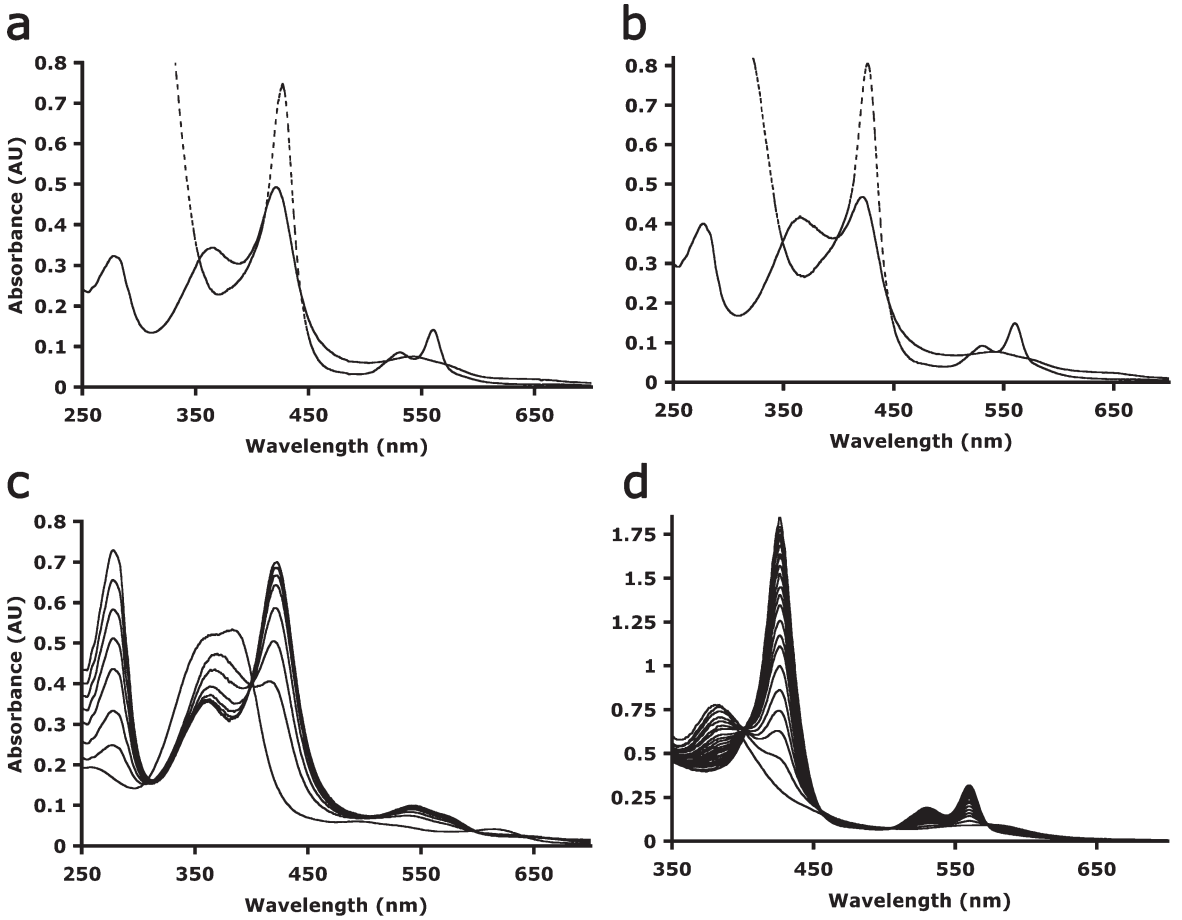

FIGURE 1: PER2 binds heme in a manner dependent on redox state. (a) UV−visible absorption spectra of PER2 (1−506) reconstituted with heme (5 μM, pH 7.5) before (—) and after (- - -) treatment with dithionite. (b) UV−visible absorption spectra of PAS A [PER2 (1−320)] reconstituted with heme (4 μM, pH 7.5) before and after treatment with dithionite. (c) Titration of ferric heme (10 μM) with PER2 (1−506) (1.5, 3, 5, 6.5, 8, 9.5, 11 μM). (d) Titration of ferrous heme (10 μM) with PER2 (1−506) (2.1, 4.2, 6.3, 8.4, 10.5, 12.6, 14.7, 16.8, 19.0, 21.1, 23.2, 25.3, 27.4, 29.5, 31.6, 33.7, 35.8, 37.9, 40.0, 43.9, 47.8, 59.5 μM).

functions with Mathematica 7.0. The reported values are the average of three independent experiments.

Electrochemistry. Glassy carbon electrodes were polished using 0.3 μm alumina slurry and repeatedly sonicated in water to remove excess alumina. Protein or heme solutions were applied to the electrode surface and incubated for 1 min to allow for adhesion. Cyclic voltammetry was performed using a CH Instruments Model 630B potentiostat, a saturated calomel reference electrode (SCE), a platinum wire as a counter electrode, and 10 mM NaCl as a supporting electrolyte. Buffer solutions were purged with nitrogen to remove oxygen prior to the beginning of experiments.

RESULTS

Heme Binds to the PAS Domains of PER2. To investigate the potential role of heme interaction with PER2 in regulating the mammalian circadian clock, we carried out a biochemical characterization of the PAS domains of PER2 with respect to heme binding. A truncated fragment of PER2 (1−506), containing both PAS A and PAS B, was overexpressed in *E. coli* BL21-(DE3) cells in LB media. Purified protein did not contain any detectable amounts of heme or any other cofactors. To ensure the availability of heme during overexpression, the heme precursor 5-aminolevulinic acid (δ-ALA) was added to the growth media; however, this also did not result in any heme incorporation into PER2.

To test whether PER2 was capable of binding heme *in vitro*, protein and cofactor were incubated together and run on a Superdex 200 (H26-60) size exclusion column. Heme coeluted with all PER2 fragments that contained the PAS domains, thereby confirming that PER2 has the capacity to bind heme. Vitamin B_{12} has been reported to compete with heme in binding to the PAS domains of PER2 (*13*). Our size exclusion assay indicated vitamin B_{12} does not bind to PER2 (1−506). As a control, FAD, a common cofactor found in other PAS domains, was tested and found also not to bind to PER2 (1−506).

Heme binding by PER2 was characterized using UV−visible absorption spectroscopy. The PER2−heme complex displayed a Soret peak at 424 nm with broad α/β peaks at 572 and 548 nm. Reduction with dithionite shifted the Soret peak to 426 nm with α/β peaks at 560 and 530 nm (Figure 1a). A truncated form of PER2 (1−320) containing only the PAS A domain had a similar spectrum to PER2 (1−506) for both ferric and ferrous states (Figure 1b). However, PAS A had a reduced capacity for heme binding (1 to 1 molar ratio of protein to heme in Figure 1b) compared to PER2 (1−506) (1 to 2 molar ratio of protein to heme in Figure 1a), demonstrating PAS A alone cannot account for all of the heme binding in PER2 (1−506). These results indicate that heme is low-spin hexacoordinate when bound to both PAS A (1−320) and PER2 (1−506). All spectra were identical to those previously reported for the PAS domains of PER2 and nPAS2, suggesting heme is bound in a similar fashion to that observed in those studies (*16*−*20*).

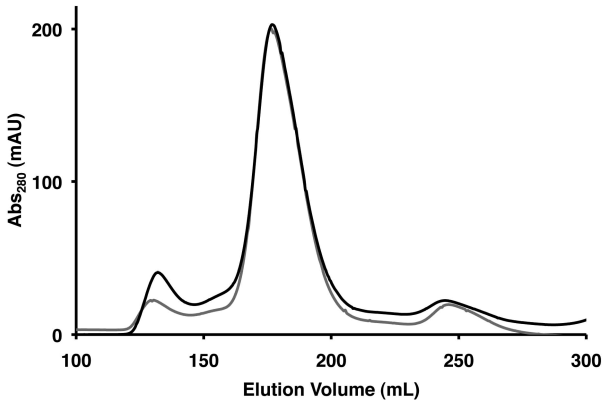

FIGURE 2: Heme binding does not affect the oligomeric state of PER2. The elution profiles of PER2 (1−506) with heme bound (black) and without heme bound (gray) are identical and indicate PER2 (1−506) forms a dimer with an apparent MW = 150 kDa (actual MW = 56 kDa).

Size Exclusion Chromatography. To determine the oligomeric state of the PAS domains of PER2, both purified PER2 (1−506) and PAS A were individually applied to a Superdex 200 column. Both PER2 (1−506) and PAS A eluted at volumes consistent with the formation of a dimer, with apparent molecular masses (MWs) of 150 kDa (actual MW = 56 kDa) and 95 kDa (actual MW = 35 kDa). The elution volume of PER2 (1−506) was identical in the absence and presence of heme, indicating no change in oligomeric state upon initial heme binding (Figure 2). Prolonged incubation of heme with PER2 formed higher order PER2 oligomers due to enhanced cysteine oxidation and formation of inter-PER2 disulfide bonds. Incubation in an anaerobic environment in the presence of reducing agents prevented disulfide formation and did not lead to higher order oligomerization.

MCD Identification of Axial Ligands for PAS A in Ferric and Ferrous Forms. Magnetic circular dichroism (MCD) spectroscopy is a useful method for determining heme coordination modes as it can identify the ligands (number and type), spin state, and oxidation state of the heme center (*29*). MCD spectra can be either positive or negative, providing greater fingerprinting capability in comparison to traditional absorption spectra, which only have positive sign features. We sought to characterize the ligand set for the isolated PAS A domain of PER2 using MCD spectroscopy. The overall shape and peak position of ferric PAS A was very similar to that of imidazole-bound ferric cytochrome P450cam, which is well-known to represent hexacoordinate Cys/imidazole ligation (*30*), as well as the recently reported MCD spectral results on butylimidazole-bound His60Cys nitrophorin 1 (H60C_NP1) (*31*) (Figure 3a). This indicates that the ligation state of the ferric heme in PAS A also features His/Cys coordination. Reduction of PAS A with sodium dithionite to ferrous PAS A results in formation of a six-coordinate low-spin complex with MCD spectral characteristics very similar to those of the deoxyferrous H93G myoglobin bis-imidazole adduct (Figure 3b), which has nitrogenous ligation in both the proximal and distal sites (*32*). Thus, unlike ferric coordination, the ferrous ligation state of PAS A is most likely bis-His. In addition, both ferrous PAS A and PER2 (1−506) are capable of binding carbon monoxide. The MCD spectra of ferrous−CO PAS A were identical to that of myoglobin with CO bound, which indicates that His and not Cys serves as the trans ligand to carbon monoxide in ferrous PAS A (*33*) (Figure 3c). We note that MCD in the wavelength range tested does not differentiate bis-His from bis-Met coordination;

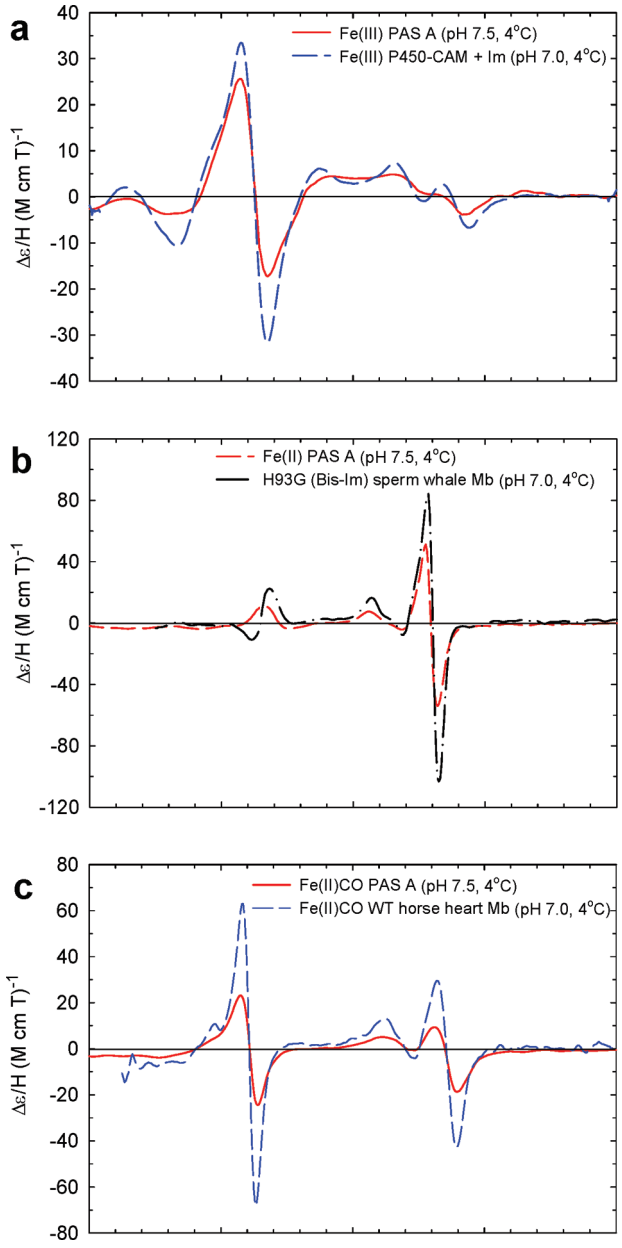

FIGURE 3: Magnetic circular dichroism spectra of ferric PAS A, ferrous PAS A, and ferrous−CO PAS A reveal ferric and ferrous hemes are bound through His-Cys and bis-His ligation, respectively. (a) MCD spectra of ferric PAS A (red) and ferric cytochrome P450−camphor with imidazole bound (blue). (b) MCD spectra of ferrous PAS A (red) and ferrous H93G sperm whale myoglobin with bis-imidazole ligation (black). (c) MCD spectra of ferrous−CO PAS A (red) and ferrous−CO wild-type horse heart myoglobin (blue).

however, analysis of the mPER2 crystal structure (*5*) did not indicate the positioning of any two Met residues capable of bis-Met coordination in PAS A or PAS B alone. Furthermore, the identification of His as the trans ligand for the ferrous−CO complex also suggests Met residues are not involved in heme coordination.

Heme Binding by PAS A and Site-Directed Mutants. Having established the PAS A ferric and ferrous heme complexes as His-Cys and bis-His coordinated, we sought to identify the specific residues acting as axial ligands. PAS A contains six histidine residues and six cysteine residues that could serve as the axial ligands for bound heme. Alignment with FixL, a heme-binding PAS domain of known structure, revealed H232 and

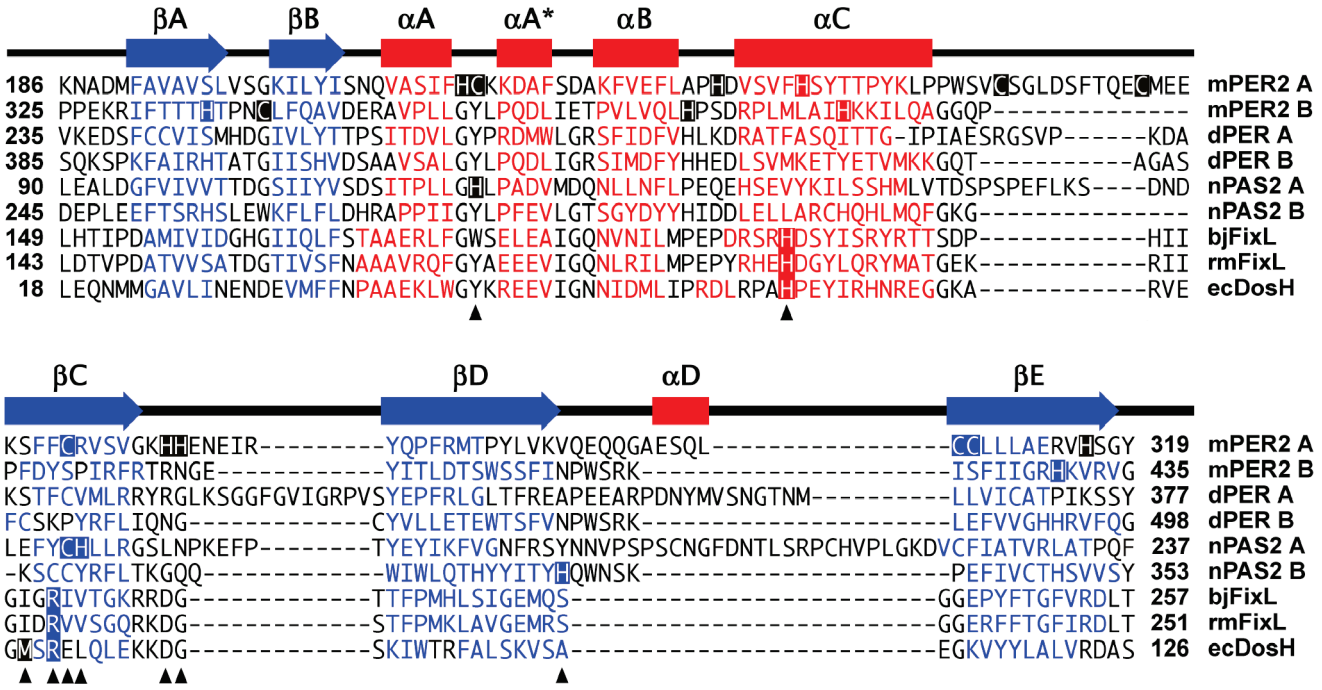

FIGURE 4: Secondary structure alignment of the PAS domains of mPER2 (PAS A, 186−319; PAS B, 325−435), dPER (PAS A, 235−377; PAS B, 385−498), nPAS2 (PAS A, 90−237; PAS B, 245−353), bjFixL (149−257), rmFixL (143−251), and ecDOS (18−126). Secondary structure information is derived from mPER2 (3GDI), dPER (1WA9), bjFixL (1DP9), rmFixL (1EW0), and ecDOS (1VB6). Jpred3 (*48*) was used to predict the secondary structure of nPAS2. α-Helices (red) and *β*-strands (blue) are colored accordingly. All cysteine and histidine residues in mPER2 are highlighted. All residues implicated in heme binding are highlighted and denoted with black triangles below. Alignments were generated with ClustalW and manually adjusted as presented.

Table 1: UV−Visible Absorption and HA_{50} Values Obtained from Heme Titrations[a]

	ferric		ferrous			
protein	Soret (nm)	*β*, α (nm)	Soret (nm)	*β*, α (nm)	ferric HA_{50}	ferrous HA_{50}
mPER2 1−506 (PAS A/B)	424	548, 572	426	530, 560	0.25	0.61
mPER2 1−320 (PAS A)	424	543, 570	426	530, 560	0.63	1.31
PAS A H214A	424	548, 572	426	530, 560	0.26	2.71
PAS A H232A	422	548, 573	426	531, 560	0.12	0.92
PAS A H238A	425	547, 572	426	529, 559	0.93	4.97
PAS A H277/278A	424	547, 572	426	530, 560	0.60	18.1
PAS A H316A	424	546, 570	426	528, 558	0.76	1.81
mPER2 972−1257	424	543, 573	426	531, 560	1.40	3.42
mPER2 129−506	424	543, 573	426	530, 560	ND	ND
mPER2 129−506 (Cys-MOD)	411	534, 567	426	529, 559	ND	ND
YqeH	409	542, 570	426	531, 560	2.63	4.76
CheAΔ289	NA	NA	426	530, 560	NA	2.72
Δ289 D371C	424	550,573	426	530, 560	6.84	1.80
YtvA	426	548, 572	428	532, 562	0.74	2.41

[a]NA = not applicable, ND = not determined.

H238 to most likely serve as the axial ligand for heme given that they hold analogous positions in the αC helix of the PAS fold compared to the heme-ligating histidine residue in FixL and ecDOS (Figure 4) (*34*−*36*). Each histidine residue in PAS A was individually mutated to an alanine in an effort to disrupt or alter heme binding.

Titration experiments were carried out with WT and mutant proteins by addition of purified protein to either free ferric or ferrous heme (Figure 1c,d). Spectral changes were monitored for a shift in Soret and α/*β* peaks, as well as for changes in relative binding potency (Table 1). We developed a method to measure the relative potency of heme binding that could account for multiple nonspecific sites. So-called HA_{50} values were calculated by taking the molar ratio of protein to heme concentration at half the maximum absorbance change in the Soret peak. This allows free heme to be the limiting factor and avoids the open-ended participation of progressively weaker binding sites at high heme concentrations. Thus HA_{50} values report on the average potency of heme binding of a specific protein and are most useful to compare closely related proteins. Changes in HA_{50} can reflect either changes in stoichiometry, binding affinity, or both. If $2 \times HA_{50} < 1$, there are multiple sites present with dissociation constants (K_D) lower than that of the free heme concentration. With $2 \times HA_{50} = 1$, one strong binding site is most likely present. With $2 \times HA_{50} > 1$, one or more sites with K_D greater than the free initial heme concentration are present. Binding affinity was

found to be redox state dependent for PAS A and PER2 (1−506), with ferric heme having a higher affinity for both proteins in comparison to ferrous heme (*19*). Although the H277/278A double mutant displayed a 10-fold reduction in HA_{50} values for ferrous heme, spectral shapes were identical to that seen in WT. This indicated there must be an alternative binding site involving a nearby histidine residue capable of substituting for H277/278. In addition, the H277/278A mutant showed no change in affinity for ferric heme. Thus, ferric and ferrous hemes preferentially bind to different sites on PAS A. Furthermore, our analysis failed to identify a specific residue responsible for heme binding.

Cysteine Modification Alters Ferric but Not Ferrous PER2 Spectra. To validate the identity of the ligand set for the ferric and ferrous PER2−heme complexes, we conducted heme titrations with PER2 protein modified with iodoacetimide. Treatment with iodoacetimide irreversibly modifies solvent-exposed cysteine residues to form a thioester ($-CH_2-S-C(=O)-$) but does not modify histidine residues. As expected, titration of heme with modified PER2 resulted in altered spectral properties for the ferric (Table 1) but not the ferrous heme−PER2 complex (Figure 5), which confirms Cys as a ligand for ferric but not ferrous heme. In addition, this result indicates that the cysteine residues responsible for heme binding in PER2 are solvent accessible, located either on the surface of PER2 or in the buried pocket accessible through solvent channels.

A C-Terminal Domain of PER2 Also Binds Heme. As a control, a C-terminal fragment of PER2, PER2 (972−1257), with no known functional role for heme binding was assayed with the above-mentioned titration method. Surprisingly, titration of free heme with PER2 (972−1257) resulted in identical spectral shifts as seen with the PAS domains of PER2. In addition, heme binding occurred with approximately the same affinity as PER2 (1−506) and PAS A with HA_{50} values of 1.40 and 3.42 for ferric and ferrous heme (Table 1).

Nonspecific Binding of Heme to Other Proteins. To test if these spectral changes were a specific property of PER2, further titration experiments were conducted with different proteins of various functions. YqeH, a GTPase from *Geobacillus stearothermophilis*, is involved in ribose biogenesis and has no known function related to heme (*27*). Addition of YqeH to ferric heme produced a Soret band at 409 nm, different from that seen with PER2, but similar to previously reported spectra of PAS A in the presence of the heavy metal mercury (*19*). YqeH contains a zinc-binding domain that could supply Cys ligands for heme iron coordination and account for the observed spectral differences compared to PER2. Reduction with dithionite shifted the Soret peak to 426 nm with α/β peaks at 560 and 530 nm, identical to that of PER2 and nPAS2 (*13*, *19*).

Second, the well-characterized histidine kinase CheA from *Thermotoga maritima* was tested for heme binding (*25*). A truncated form of CheA (Δ289) that contains the core dimerization, kinase, and regulatory domains but lacks cysteine residues was tested for heme binding. Interestingly, titration of ferric heme with Δ289 did not produce any change in peak shape but did decrease the extinction coefficient of free heme at the absorbance maximum (Figure 6a). However, spectral shifts identical to PER2 and YqeH were seen when Δ289 was added to ferrous heme (Figure 6b). Δ289 titration results demonstrate that cysteine is not required for binding ferrous heme but is required to produce the characteristic spectral changes with ferric heme.

In an attempt to induce the spectral changes in CheA observed on addition of PER2 to ferric heme, a non-native cysteine was introduced at a solvent-exposed surface residue of CheA Δ289 (Δ289-D371C). The addition of Δ289-D371C to ferric heme produced a shoulder on the Soret peak at longer wavelength (Figure 6c). Difference spectra identified this shoulder as a Soret peak growing in at 424 nm, matching the heme-binding signal observed for PER2 (Figure 6d). Thus, addition of a non-native surface cysteine residue produced spectral changes identical to PER2 but did so with a much lower binding affinity.

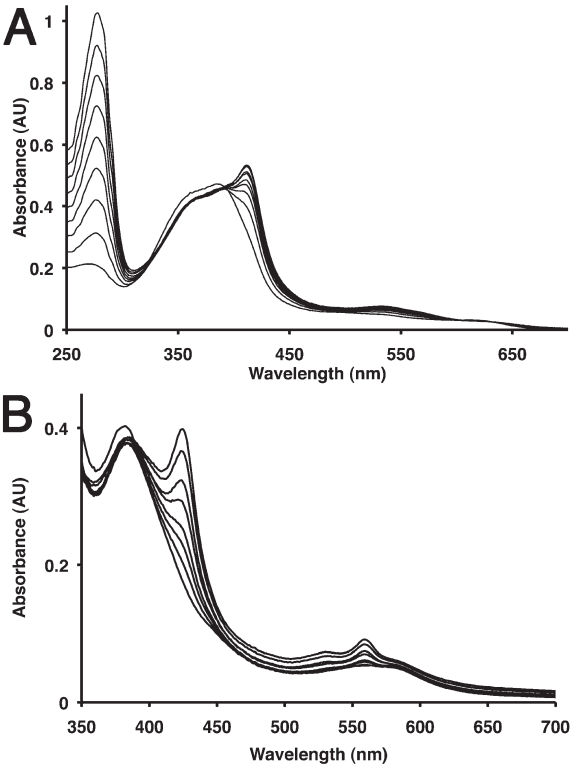

FIGURE 5: Cysteine modification alters the ferric but not the ferrous heme PER2 spectra. (A) Titration of ferric heme (8.3 μM) with PER2 (129−506) modified with iodoacetamide (0, 6, 10, 14, 18, 22, 26, 30, 34 μM). Cysteine modification alters the position of the Soret peak, shifting it to 410 nm compared to unmodified PER2 with a Soret peak at 422 nm. (B) Titration of ferrous heme (8.3 μM) with PER2 (129−506) modified with iodoacetamide (0, 4.1, 8.2, 12.4, 24.7, 37, 58, 78 μM) with a Soret peak growing in at 426 nm identical to unmodified PER2.

PAS domains, such as PER2, typically bind cofactors in a pocket primarily formed by the central β-sheet, the αB and αC helices, and the αB−αC loop (*37*). YtvA is a PAS domain protein that binds flavin mononucleotide (FMN) in this pocket (*26*). Since YtvA contains a native cofactor, we sought to test whether YtvA could also bind heme while still maintaining FMN in its binding pocket. YtvA was first photobleached to maintain a constant FMN absorbance and induce a covalent link between the cofactor and protein (*26*). Titration experiments were carried out with both ferric and ferrous heme. After subtraction of the absorbance due to FMN the resulting ferric and ferrous spectra were found to be identical to PER2 (Figure 7). The binding affinity of heme to YtvA was comparable to that of PER2 (1−506) and PAS A with HA_{50} values of 0.74 and 2.41 for ferric and ferrous heme, respectively (Table 1). Due to the presence of covalently bound FMN, heme cannot bind in the hydrophobic pocket of the YtvA PAS domain and must therefore be interacting with residues on the surface of the protein.

Dissociation Rate Constant(s) of PER2 and Other Proteins Indicate Nonspecificity. HA_{50} values provide a qualitative

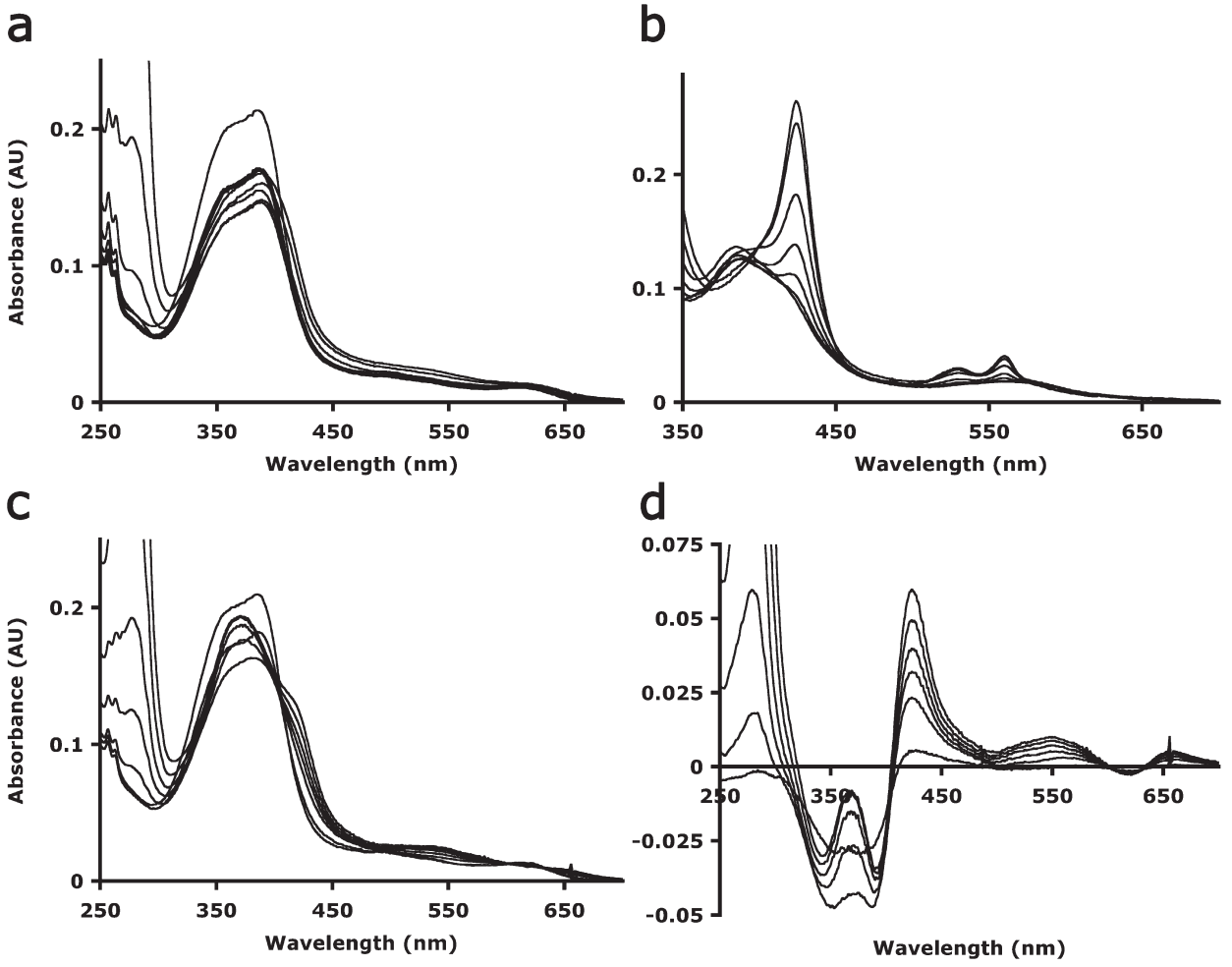

FIGURE 6: Heme binds to the chemotaxis kinase CheA. (a) Titration of ferric heme (4 μM) with CheA (0, 0.23, 0.45, 1.1, 3.5, 11.6, 35 μM). (b) Titration of ferrous heme (4 μM) with CheA (0, 0.45, 2.3, 5.8, 11.6, 23, 46.5 μM). (c) Titration of ferric heme (4 μM) with CheA D371C variant (0, 0.5, 2.5, 6.4, 12.8, 25, 45 μM). (d) Difference spectra from panel c.

means to compare relative heme-binding affinities under the same conditions but are complicated by the possibility of different heme-binding stoichiometries and variable binding affinities of multiple sites. To further verify heme binding to PER2 as nonspecific, we sought to evaluate binding affinities for heme. Major differences in heme-binding affinity could be due to differences in the association and/or dissociation rate constants. For association experiments, CO−heme produces a more monomeric form of free heme suitable for kinetic analysis. However, it has been shown that the heme−CO association rate constant is independent of protein structure (*38*) and overall affinity is determined by the dissociation rate constant. Previous work (Table 2) determined the dissociation rate constant of PER2 1−327 (PAS A) as 6.3×10^{-4} s^{-1} (*19*), compared to the specific binding of sperm whale myoglobin, $k_{off} = 8.4 \times 10^{-7}$ s^{-1} (*38*), nonspecific binding of human BSA, $k_{off} = 1.1 \times 10^{-2}$ s^{-1} (*38*), and bHLH-PAS A domains of the putative heme-binding CO sensor nPAS2, $k_{off} = 5.3 \times 10^{-3}$ s^{-1} (*18*). To add to such comparisons, we determined and compared the dissociation rate constants for PER2 and the other proteins that display similar heme-binding spectral properties.

We measured the dissociation rate constant of mPER2 1−320 to be 1.6×10^{-3} s^{-1} when fit as a first-order process (Table 2, Figure 8), which is comparable to the previously determined value by Kitanishi et al. (*19*). However, both our data and that reported by Kitanishi et al. (*19*) were not fit well by a single exponential process. A biexponential process produces much better agreement with the experimental data (Table 2, Figure 8). This indicates there are at least two binding sites or two sets of binding sites for heme on PER2 with different affinities. All proteins tested had similar rate constants for heme dissociation and were fit well as bimolecular processes (Table 2). As a control, we tested a recently identified FixL-like heme-binding PAS protein from *Pseudomonas aeruginosa* that copurifies with bound heme (*39*). In contrast, heme dissociation from the FixL-like PAS domain was a single process, and the dissociation rate constant was considerably lower than PER2 at 6.9×10^{-5} s^{-1} (Table 2).

Electrochemistry. Protein−film voltammetry was used to evaluate the redox properties of the PER2−heme complex and thereby provide information on the local heme environment bound to PER2. A solution of the concentrated PER2−heme complex was applied to a freshly polished glassy carbon electrode to generate a protein film immobilized on the electrode surface. Cyclic voltammograms of the purified PER2−heme complex displayed a reduction peak at $E^\circ = -396$ mV relative to SCE, which is characteristic of solvent-exposed heme bound to a protein surface (*40*) (Figure 9). Subsequent scanning to higher potentials did not reveal a corresponding oxidation reaction, which may indicate that ferrous heme is no longer in electrochemical contact with the electrode surface. In comparison, free heme immobilized on the electrode surface displayed coupled reduction and oxidation peaks with $E^\circ = -372$ mV (Figure 9). This confirms that the

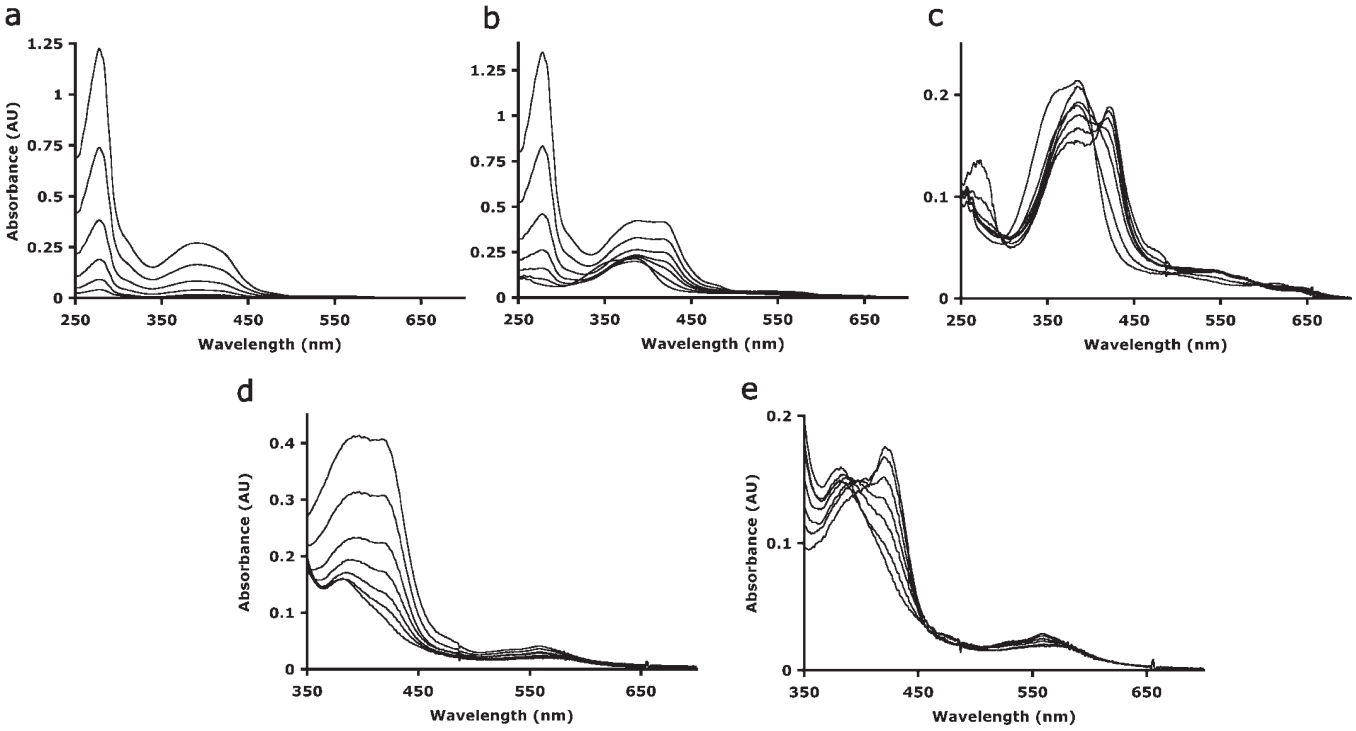

FIGURE 7: Addition of YtvA induces spectral changes to ferric and ferrous heme. (a) UV−visible absorption spectra of YtvA (0, 1.2, 3, 6, 12, 24, and 42 μM) after photobleaching. (b) Titration of ferric heme (4 μM) with YtvA (0, 1.2, 3, 6, 12, 24, and 42 μM). (c) Absorption spectra from titration of ferric heme with YtvA after subtraction of FMN absorbance. (d) Titration of ferrous heme (4 μM) with YtvA (0, 1.2, 3, 6, 12, 24, and 42 μM). (e) UV−visible absorption spectra from titration of ferrous heme with YtvA after subtraction of FMN absorption.

Table 2: Heme Dissociation Rate Constants for mPER2 and Other Heme-Binding Proteins

protein	k_{off} (s^{-1})[a]	k_{off1} (s^{-1})[b]	k_{off2} (s^{-1})[b]	ref
mPER2 1−320	1.6×10^{-3}	7.8×10^{-3}	4.8×10^{-4}	this work
mPER2 1−506	3.1×10^{-3}	7.6×10^{-3}	2.4×10^{-4}	this work
mPER2 972−1257	7.2×10^{-4}	1.2×10^{-3}	4.3×10^{-3}	this work
YtvA	4.8×10^{-4}	1.6×10^{-3}	1.2×10^{-4}	this work
YqeH	5.0×10^{-4}	2.2×10^{-2}	4.0×10^{-4}	this work
FixL-like PAS	6.9×10^{-5}			this work
mPER2 1−327	6.3×10^{-4}			*19*
NPAS2 (bHLH-PAS A)	5.3×10^{-3}			*18*
Sw Mb[c]	8.4×10^{-7}			*38*
Hb α-subunit[c]	7.1×10^{-6}			*38*
BSA (human)[c]	1.1×10^{-2}			*38*

[a]Rate constants were calculated assuming a single phase. [b]Rate constants were calculated assuming a two-step process. [c]Rate constants are given for 20 °C. All other rate constants refer to 25 °C.

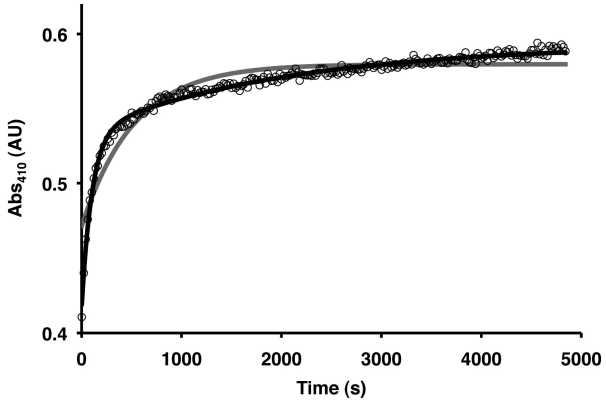

FIGURE 8: Heme dissociation from PER2 occurs from multiple sites. Heme transfer from PER2 (1−320) to H64Y/V68F apomyoglobin was measured as an increase in the absorbance at 410 nm in 0.2 M sodium phosphate, pH 7.0, and 0.45 M sucrose at 25 °C. Rate constants were calculated by analyzing the data in terms of both single exponential (gray) and biexponential processes (black) (Table 2). The data for PER2 and other proteins were best represented by a biexponential process indicating multiple binding sites with different affinities.

reduction peak for the PER2−heme complex is not due to free heme directly binding to the electrode surface. In the case of the heme−protein complex, reduction may cause heme to dissociate from PER2 due to PER2's lower binding affinity for ferrous heme; thus no corresponding oxidation peak is observed. However, there is also the possibility that the initial reduction peak was due to catalytic reduction of a small amount of oxygen that could not be purged from the protein−heme complex. Such a scenario would also preclude observation of an oxidation peak. Although these two possibilities are difficult to distinguish, they both are consistent with heme being bound to a solvent-exposed site on PER2.

DISCUSSION

Potential roles for heme in the regulation of the circadian clock continue to emerge (*13*, *16*−*22*, *41*−*43*). Direct heme interactions have been suggested to regulate the stability and transcriptional activity of the clock components PER2 and nPAS2. However, much of the supporting evidence has been based upon biochemical assays of purified proteins (*16*−*20*, *41*, *42*). To examine the biological relevance of these *in vitro* assays, we tested a number of well-characterized proteins with no role for heme binding. Interestingly, all of these proteins were found to bind heme in a manner comparable to PER2. This then raises the question: Is heme binding to PER2 biologically relevant?

Our initial characterization of PER2 confirmed that the PAS domains bind heme, in agreement with a previous report (*19*).

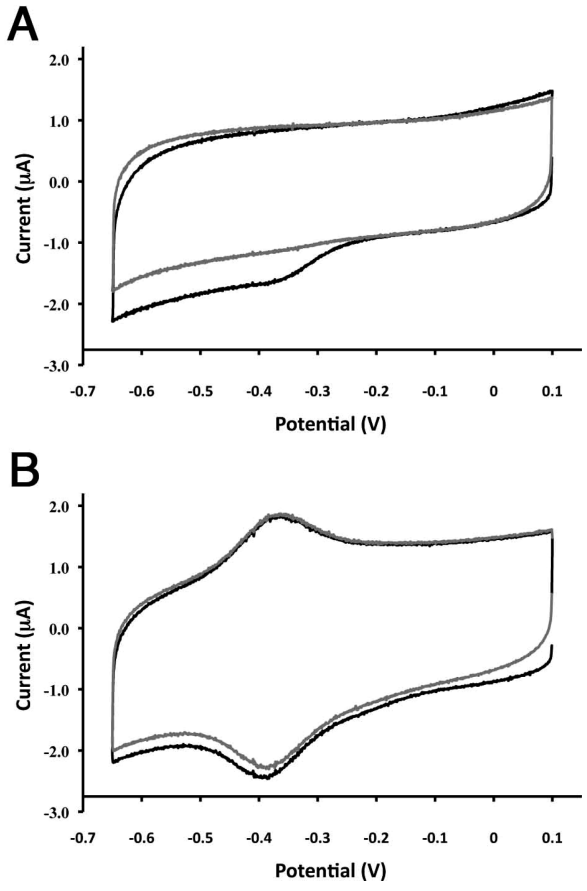

FIGURE 9: Electrochemistry of the PER2−heme complex. (A) Cyclic voltammogram of the PER2−heme complex immobilized on a glassy carbon electrode. (B) Cyclic voltammogram of heme immobilized on a glassy carbon electrode under the same conditions as in (A). Black and gray traces denote the first and second potential sweeps. All scan rates were 100 mV/s.

PER2 formed a stronger association with ferric heme compared to ferrous heme. Electrochemical analysis of the PER2−heme complex suggests that heme may dissociate from PER2 upon reduction, consistent with redox-state dependent binding location and affinity. With the methods of UV−visible absorption and MCD spectroscopy we identified that the PAS A domain of PER2 binds ferric heme as His-Cys coordinated and ferrous heme as bis-His coordinated. Site-directed mutagenesis identified histidine residues 277 and 278 as the primary histidine axial ligands to ferrous heme. Replacement of these residues with alanine only affected the affinity for ferrous heme but not ferric heme. Although the affinity for ferrous heme was much less in the double mutant, the same changes in spectral features were observed as with the native protein. Thus, heme binding to PER2 can occur at multiple sites.

We then examined heme binding to a number of previously characterized proteins with no known role for heme binding. As with PER2 and nPAS2, overexpression of these proteins in *E. coli* did not result in any heme incorporation. However, our *in vitro* assay determined all proteins tested were capable of binding heme. All proteins assayed displayed binding affinities for heme similar to PER2 and produced identical UV−visible absorption spectra (Table 1). These results question the effectiveness of spectral assays of this type to differentiate between specific and nonspecific heme binding.

Rate constants for heme dissociation were in the same range for the PER2 PAS domains and the control proteins, strongly indicating that heme binding to PER2 is nonspecific (Table 2). Furthermore, the dissociation rate constants are high compared to the specific heme-binding proteins Sw Mb, Hb α-subunit, and FixL-like PAS. Multiple nonspecific sites were confirmed by fitting the experimental data using a biexponential decay. For the specific heme-binding FixL-like PAS domain, heme dissociation was modeled well as a single first-order process.

Moreover, the identify and type of axial ligand coordination in PER2 were dependent on the redox state of heme, which indicates that ferric and ferrous heme bind to different sites on the protein. The presence of a cysteine residue in the polypeptide sequence is absolutely required to bind ferric heme as evidenced by a Soret peak at 424 nm and broad α/β peaks at 572 and 548 nm. If no surface cysteine residues are present, the addition of protein to ferric heme will not induce any spectral changes indicative of heme binding, as observed for CheA Δ289. However, with the introduction of a surface cysteine residue into Δ289 the characteristic heme-binding signals were recapitulated. Thus, any solvent-exposed cysteine is likely capable of binding ferric heme and generating the associated spectral response. Modification of solvent-exposed cysteine residues altered the ferric spectra of PER2, indicating that ligand binding does occur on the protein surface. Alternatively, a surface cysteine residue is not required to bind ferrous heme, as native Δ289 and cysteine-modified PER2 displayed the usual spectral changes upon ferrous heme titration. Hence, surface histidine residues are sufficient to produce the typical ferrous spectra with the Soret peak at 426 nm and sharp α/β peaks at 560 and 530 nm. Cys-His coordination for ferric heme and bis-His coordination for ferrous heme were confirmed by MCD spectroscopy. MCD experiments also verify that a cysteine or methionine residue is not involved in binding ferrous heme with histidine serving as the trans axial ligand to bound CO in ferrous PAS A. Redox-state dependent binding has been reported for the putative novel heme-binding motif, Ser-Cys^{841}-Pro-Ala, of PER2 in a region outside the PER2 PAS domains (*20*). UV−vis spectral changes found that this motif bound ferric heme (with spectra identical to the PER2 PAS domains) but was unable to bind ferrous heme. The behavior of this Cys-containing motif is consistent with the same nonspecific heme-binding displayed by the PER2 PAS domains where ferric heme-binding is Cys-His coordinate and ferrous heme-binding is bis-His coordinate.

To analyze potential heme-binding modes for the PAS domains of PER2 and nPAS2, we examined a secondary structure-based alignment with other PAS domains of known structure and heme-binding function (Figure 4). FixL and ecDOS are bacterial heme-binding PAS domains whose axial ligand is a highly conserved histidine residue found in the αC helix of the PAS fold (*34*−*36*). Although PER2 and nPAS2 do not conserve this histidine residue, it is plausible that they harbor a different histidine residue that is specific for heme. However, sequence alignments failed to identify any conserved residues that might point to a novel heme-binding motif shared between PER2 and nPAS2. Analysis of the mPER2 PAS domain structure (*5*) found that all proposed heme ligation residues are positioned at a solvent-exposed site, consistent with our biochemical analysis (Figure 10). In addition, we have shown that when the PAS domain pocket is blocked by a cofactor, such as FMN in YtvA, the PAS domains still bind heme in a manner similar to the PER2 protein.

The recent crystal structure of the mPER2 PAS domains (PDB code 3GDI) allows for a structural analysis of potential heme-binding ligands (*5*). A previous study identified Cys215 and Cys270 in PAS A to be important for ferric heme interactions (*19*). A double mutant, C215A/C270A, resulted in spectral

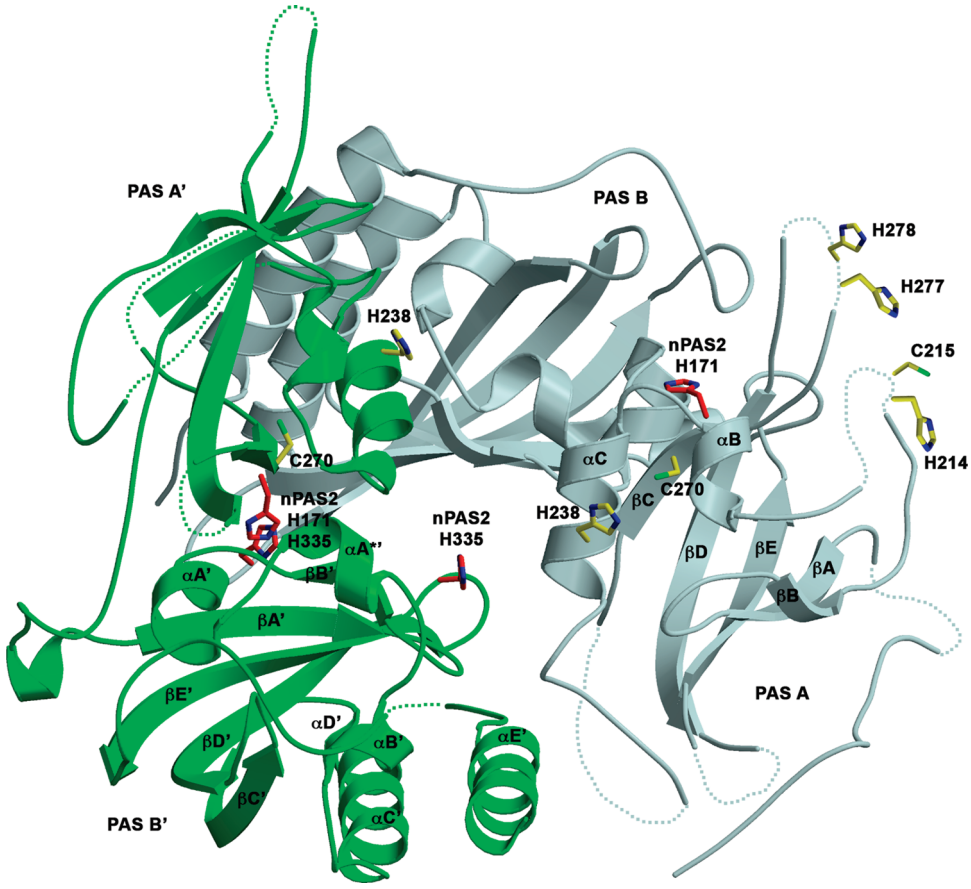

FIGURE 10: mPER2 structure with the location of possible heme-binding residues. Ribbon representation of mPER2 PAS A/B dimer (3GDI): molecule 1 (PAS A and PAS B); molecule 2 (PAS A′ and PAS B′). Side chains are shown for residues H214, C215, H238, C270, H277, and H278 in mPER2 (yellow) and C170, H171, and H335 in nPAS2 (red). H119 of nPAS2 is not shown but corresponds to C215 of PER2. Residues with missing density are depicted as a dotted line and were manually drawn. The secondary structure elements of the PAS fold are labeled for PAS A and PAS B′.

perturbations of ferric heme bound to PER2 PAS A, as analyzed by UV−visible absorption, electron paramagnetic resonance (EPR), and resonance Raman (RR) spectroscopy. However, the double mutant displayed identical spectra for ferrous and ferrous−CO heme iron states compared to wild type. All UV−visible absorption, EPR, and RR spectra of the single Cys mutants were identical to wild type. Nonetheless, Cys215 was proposed as the primary heme interacting residue for ferric heme because the C215A mutant displayed an altered heme circular dichroism (CD) spectrum, whereas the C270A mutant did not (*19*). Cys215 is located on a surface-exposed region of PAS A that also contains His214, His277, and His278, all in close proximity and thus would be capable of both bis-His and His-Cys ligation (Figure 10). H277/278A and H214A PAS A mutants have lowered affinities for ferrous heme, consistent with this as the primary site for heme interaction in PAS A. Furthermore, given the position of Cys270 on the buried face of the PAS A β-sheet, a Cys-His heme coordination mode involving Cys270 could only be possible with substantial structural distortion of the PAS A domain. Other interaction sites capable of bis-His and His-Cys ligation may be possible in a PAS A/A homodimer. In the crystal structure of the PAS domains of PER2 (*5*), dimerization is mediated by the PAS B domains with no observed interaction between the PAS A domains. But, truncation of PAS B allows the PAS A domains to dimerize (*19*), as determined by size exclusion chromatography.

The binding of ferrous heme to PER2 also shows many characteristics similar to those of *de novo* designed heme proteins. Rojas et al. (*44*) reported the heme-binding properties of 30 different peptides predicted to fold into four-helix bundles. This library of proteins contained on average 4.3 histidine residues and 4.9 methionine residues capable of heme ligation. None of the proteins contained cysteine residues. The authors found that 15 of 30 sequences bound heme similarly to *b*-type cytochromes with a Soret peak at 412 nm for ferric heme and a broad α/β band centered around 550 nm. Upon reduction the Soret peak was shifted to 426 nm with sharp α and β peaks at 560 and 530 nm, respectively, identical to that observed for PER2. Another study (*45*) used a combinatorial synthesis approach to design and test 426 amphiphilic antiparallel four-helix bundles. Of the 426 proteins assayed, 399 were found to bind heme and give rise to a Soret band at 414 nm for the ferric state and a *b*-type cytochrome spectrum, identical to PER2 and proteins described by Rojas et al. (*44*), for the ferrous state.

From the variety of protein folds assayed it is clear that the spectral signals indicative of heme binding do not require a specific mode of interaction between heme and a conserved protein architecture. Any polypeptide sequence containing both a cysteine and a histidine residue is sufficient to induce the spectral changes observed for PER2. Considering the low solubility of free heme, it is most likely that binding occurs at surface histidine and cysteine residues aided by hydrophobic patches on the surface of each protein. Heme has long been known to form homooligomers in aqueous solution (*23*). Additionally, heme binds nonspecifically to phospholipid bilayers and associates with membrane skeletal proteins due to its high

hydrophobicity (*46*, *47*). Given the evidence against the specificity of heme binding to PER2, we urge caution in the interpretation of results from previous *in vitro* assays and question the biological relevance of heme binding in relation to the clock protein PER2. We note that the *in vitro* heme interactions observed for nPAS2 are very similar to those of PER2, and in our view, this also calls into question their biological relevance.

If heme binding to PER2 and nPAS2 is not biologically relevant, the question remains, how does heme feed back into the clock to coordinate circadian timing (*13*, *14*, *16*, *19*−*22*)? The identification of heme as the ligand for the nuclear receptors REV-erbα and REV-erb*β* may provide this connection (*21*, *22*). Both REV-erbα and REV-erb*β* bind heme specifically through their ligand-binding domains (LBDs). Heme binding causes REV-erbα to recruit the nuclear receptor corepressor−histone deacetylase 3 (NCoR−HDAC3) complex, which results in decreased transcription of bMAL1, a necessary component for active transcription of clock and clock-controlled genes (*21*, *22*). Noteworthy is the fact that overexpression of the REV-erb LBDs in *E. coli* produces proteins that purify with bound heme and display UV−visible absorption spectra different from those of PER2 and nPAS2. In contrast, there are no reports of any purified fragment of nPAS2 or PER2 protein containing heme after overexpression in *E. coli*. In all cases PER2 and nPAS2 must be reconstituted *in vitro* with free hemin (*16*−*20*, *41*, *42*). PER2 has been shown to bind to heme immobilized on a heme−agarose column (*13*, *20*). In light of the evidence presented here, this interaction likely represents nonspecific heme binding on the surface of the PER2 protein and does not involve the buried hydrophobic cavity of the PAS core. To date there has been no spectral or other evidence from PER2 or nPAS2 purified from mammalian cell lines that indicate PER2 or nPAS2 interacts with heme. Given that *in vitro* heme binding to nPAS2 and PER2 is likely nonspecific, heme influence over the mammalian circadian clock is most likely dominated by its interaction with the Rev-erb's or other factors yet to be identified.

ACKNOWLEDGMENT

The authors thank Dr. John S. Olson and Eileen Singleton (Rice University) for generously providing H64Y/V68F myoglobin protein used for heme dissociation experiments. We also thank Heather King, Michael Young, and Lino Saez (Rockefeller University) for providing mPER2 DNA, which served as a PCR template, Kylie Watts (Loma Linda University) for supplying Aer2 DNA, Dr. Masanori Sono (University of South Carolina) for help in interpreting the MCD spectra, and Kevin Hoke (Berry College) for helpful discussions of electrochemical data.

REFERENCES

1. Reppert, S. M., and Weaver, D. R. (2002) Coordination of circadian timing in mammals. *Nature 418*, 935–941.
2. Harms, E., Kivimae, S., Young, M. W., and Saez, L. (2004) Post-transcriptional and posttranslational regulation of clock genes. *J. Biol. Rhythms 19*, 361–373.
3. Lowrey, P. L., and Takahashi, J. S. (2004) Mammalian circadian biology: Elucidating genome-wide levels of temporal organization. *Annu. Rev. Genomics Hum. Genet. 5*, 407–441.
4. Young, M. W., and Kay, S. A. (2001) Time zones: A comparative genetics of circadian clocks. *Nat. Rev. Genet. 2*, 702–715.
5. Hennig, S., Strauss, H. M., Vanselow, K., Yildiz, O., Schulze, S., Arens, J., Kramer, A., and Wolf, E. (2009) Structural and functional analyses of PAS domain interactions of the clock proteins *Drosophila* PERIOD and mouse PERIOD2. *PLoS Biol. 7*, 836–853.
6. Gillesgonzalez, M. A., and Gonzalez, G. (1993) Regulation of the kinase-activity of heme protein Fixl from the 2-component system Fixl/Fixj of *Rhizobium meliloti*. *J. Biol. Chem. 268*, 16293–16297.
7. Zoltowski, B. D., Schwerdtfeger, C., Widom, J., Loros, J. J., Bilwes, A. M., Dunlap, J. C., and Crane, B. R. (2007) Conformational switching in the fungal light sensor vivid. *Science 316*, 1054–1057.
8. Yildiz, O., Doi, M., Yujnovsky, I., Cardone, L., Berndt, A., Hennig, S., Schulze, S., Urbanke, C., Sassone-Corsi, P., and Wolf, E. (2005) Crystal structure and interactions of the PAS repeat region of the *Drosophila* clock protein PERIOD. *Mol. Cell 17*, 69–82.
9. Kewley, R. J., Whitelaw, M. L., and Chapman-Smith, A. (2004) The mammalian basic helix-loop-helix/PAS family of transcriptional regulators. *Int. J. Biochem. Cell Biol. 36*, 189–204.
10. Scheuermann, T. H., Tomchick, D. R., Machius, M., Guo, Y., Bruick, R. K., and Gardner, K. H. (2009) Artificial ligand binding within the HIF2 alpha PAS-B domain of the HIF2 transcription factor. *Proc. Natl. Acad. Sci. U.S.A. 106*, 450–455.
11. Erbel, P. J. A., Card, P. B., Karakuzu, O., Bruick, R. K., and Gardner, K. H. (2003) Structural basis for PAS domain heterodimerization in the basic helix-loop-helix-PAS transcription factor hypoxia-inducible factor. *Proc. Natl. Acad. Sci. U.S.A. 100*, 15504–15509.
12. Morais Cabral, J. H., Lee, A., Cohen, S. L., Chait, B. T., Li, M., and Mackinnon, R. (1998) Crystal structure and functional analysis of the HERG potassium channel N terminus: A eukaryotic PAS domain. *Cell 95*, 649–655.
13. Kaasik, K., and Lee, C. C. (2004) Reciprocal regulation of haem biosynthesis and the circadian clock in mammals. *Nature 430*, 467–471.
14. Zheng, B. H., Albrecht, U., Kaasik, K., Sage, M., Lu, W. Q., Vaishnav, S., Li, Q., Sun, Z. S., Eichele, G., Bradley, A., and Lee, C. C. (2001) Nonredundant roles of the mPer1 and mPer2 genes in the mammalian circadian clock. *Cell 105*, 683–694.
15. Panda, S., Antoch, M. P., Miller, B. H., Su, A. I., Schook, A. B., Straume, M., Schultz, P. G., Kay, S. A., Takahashi, J. S., and Hogenesch, J. B. (2002) Coordinated transcription of key pathways in the mouse by the circadian clock. *Cell 109*, 307–320.
16. Dioum, E. M., Rutter, J., Tuckerman, J. R., Gonzalez, G., Gilles-Gonzalez, M. A., and McKnight, S. L. (2002) NPAS2: A gas-responsive transcription factor. *Science 298*, 2385–2387.
17. Koudo, R., Kurokawa, H., Sato, E., Igarashi, J., Uchida, T., Sagami, I., Kitagawa, T., and Shimizu, T. (2005) Spectroscopic characterization of the isolated heme-bound PAS-B domain of neuronal PAS domain protein 2 associated with circadian rhythms. *FEBS J. 272*, 4153–4162.
18. Mukaiyama, Y., Uchida, T., Sato, E., Sasaki, A., Sato, Y., Igarashi, J., Kurokawa, H., Sagami, I., Kitagawa, T., and Shimizu, T. (2006) Spectroscopic and DNA-binding characterization of the isolated heme-bound basic helix-loop-helix-PAS-A domain of neuronal PAS protein 2 (NPAS2), a transcription activator protein associated with circadian rhythms. *FEBS J. 273*, 2528–2539.
19. Kitanishi, K., Igarashi, J., Hayasaka, K., Hikage, N., Saiful, I., Yamauchi, S., Uchida, T., Ishimori, K., and Shimizu, T. (2008) Heme-binding characteristics of the isolated PAS-A domain of mouse Per2, a transcriptional regulatory factor associated with circadian rhythms. *Biochemistry 47*, 6157–6168.
20. Yang, J. H., Kim, K. D., Lucas, A., Drahos, K. E., Santos, C. S., Mury, S. P., Capelluto, D. G. S., and Finkielstein, C. V. (2008) A novel heme-regulatory motif mediates heme-dependent degradation of the circadian factor period 2. *Mol. Cell. Biol. 28*, 4697–4711.
21. Raghuram, S., Stayrook, K. R., Huang, P. X., Rogers, P. M., Nosie, A. K., McClure, D. B., Burris, L. L., Khorasanizadeh, S., Burris, T. P., and Rastinejad, F. (2007) Identification of heme as the ligand for the orphan nuclear receptors REV-ERB alpha and REV-ERB beta. *Nat. Struct. Mol. Biol. 14*, 1207–1213.
22. Yin, L., Wu, N., Curtin, J. C., Qatanani, M., Szwergold, N. R., Reid, R. A., Waitt, G. M., Parks, D. J., Pearce, K. H., Wisely, G. B., and Lazar, M. A. (2007) Rev-erb alpha, a heme sensor that coordinates metabolic and circadian pathways. *Science 318*, 1786–1789.
23. Brown, S. B., Dean, T. C., and Jones, P. (1970) Aggregation of ferrihaems—Dimerization and protolytic equilbria of protoferrihaem and deuteroferrihaem in aqueous solution. *Biochem. J. 117*, 733–&.
24. Travascio, P., Li, Y. F., and Sen, D. (1998) DNA-enhanced peroxidase activity of a DNA aptamer-hemin complex. *Chem. Biol. 5*, 505–517.
25. Bilwes, A. M., Alex, L. A., Crane, B. R., and Simon, M. I. (1999) Structure of CheA, a signal-transducing histidine kinase. *Cell 96*, 131–141.
26. Moglich, A., and Moffat, K. (2007) Structural basis for light-dependent signaling in the dimeric LOV domain of the photosensor YtvA. *J. Mol. Biol. 373*, 112–126.

27. Sudhamsu, J., Lee, G. I., Klessig, D. F., and Crane, B. R. (2008) The structure of YqeH an AtNOS1/AtNOA1 ortholog that couples GTP hydrolysis to molecular recognition. *J. Biol. Chem. 83*, 32968–32976.
28. Hargrove, M. S., Singleton, E. W., Quillin, M. L., Ortiz, L. A., Phillips, G. N., Olson, J. S., and Mathews, A. J. (1994) His(64)(E7)-]Tyr apomyoglobin as a reagent for measuring rates of hemin dissociation. *J. Biol. Chem. 269*, 4207–4214.
29. Cheek, J., and Dawson, J. H. (2000) Handbook of porphyrins and related macrocycles, Vol. *7*, Academic Press, New York.
30. Dawson, J. H., Andersson, L. A., and Sono, M. (1982) Spectroscopic investigations of ferric cytochrome P-450-cam ligand complexes—Identification of the ligand trans to cysteinate in the native enzyme. *J. Biol. Chem. 257*, 3606–3617.
31. Vetter, S. W., Terentis, A. C., Osborne, R. L., Dawson, J. H., and Goodin, D. B. (2009) *J. Biol. Inorg. Chem. 14*, 179–191.
32. Du, J., Sono, M., and Dawson, J. H. (2008) The proximal and distal pockets of the H93G myoglobin cavity mutant bind identical ligands with different affinities: Quantitative analysis of imidazole and pyridine binding. *Spectroscopy 22*, 123–141.
33. Collman, J. P., Sorrell, T. N., Dawson, J. H., Trudell, J. R., Bunnenberg, E., and Djerassi, C. (1976) Magnetic circular-dichroism of ferrous carbonyl adducts of cytochromes P-450 and P-420 and their synthetic models—Further evidence for mercaptide as 5th ligand to iron. *Proc. Natl. Acad. Sci. U.S.A. 73*, 6–10.
34. Key, J., and Moffat, K. (2005) Crystal structures of deoxy and CO-bound bjFixLH reveal details of ligand recognition and signaling. *Biochemistry 44*, 4627–4635.
35. Miyatake, H., Mukai, M., Park, S. Y., Adachi, S., Tamura, K., Nakamura, H., Nakamura, K., Tsuchiya, T., Iizuka, T., and Shiro, Y. (2000) Sensory mechanism of oxygen sensor FixL from *Rhizobium meliloti*: Crystallographic, mutagenesis and resonance Raman spectroscopic studies. *J. Mol. Biol. 301*, 415–431.
36. Suquet, C., Park, H. J., Kang, C. H., and Satterlee, J. D. (2005) The X-ray crystal structures of oxy- and deoxy-EcDos heme domains indicate that signal initiation-propagation is conveyed by secondary structure conformational changes. *Biophys. J. 88*, 390A–390A.
37. Gilles-Gonzalez, M. A., and Gonzalez, G. (2005) Heme-based sensors: Defining characteristics, recent developments, and regulatory hypotheses. *J. Inorg. Biochem. 99*, 1–22.
38. Hargrove, M. S., Barrick, D., and Olson, J. S. (1996) The association rate constant for heme binding to globin is independent of protein structure. *Biochemistry 35*, 11293–11299.
39. Airola, M. V., Watts, K. J., Bilwes, A. M., and Crane, B. R. (2010) Structure of concatenated HAMP domains provides a mechanism for signal transduction. *Structure 18*, 436–448.
40. Reedy, C. J., Elvekrog, M. M., and Gibney, B. R. (2008) Development of a heme protein structureelectrochemical function database. *Nucleic Acids Res. 36*, D307–D313.
41. Ishida, M., Ueha, T., and Sagami, I. (2008) Functional analysis of heme-PAS domain mutants of NPAS2: Transcriptional activity and DNA-binding activity. *FEBS J. 275*, 130–130.
42. Ishida, M., Ueha, T., and Sagami, I. (2008) Effects of mutations in the heme domain on the transcriptional activity and DNA-binding activity of NPAS2. *Biochem. Biophys. Res. Commun. 368*, 292–297.
43. Rogers, P. M., Ying, L., and Burris, T. P. (2008) Relationship between circadian oscillations of Rev-erb alpha expression and intracellular levels of its ligand, heme. *Biochem. Biophys. Res. Commun. 368*, 955–958.
44. Rojas, N. R. L., Kamtekar, S., Simons, C. T., McLean, J. E., Vogel, K. M., Spiro, T. G., Farid, R. S., and Hecht, M. H. (1997) De novo heme proteins from designed combinatorial libraries. *Protein Sci. 6*, 2512–2524.
45. Rau, H. K., DeJonge, N., and Haehnel, W. (2000) Combinatorial synthesis of four-helix bundle hemoproteins for tuning of cofactor properties. *Angew. Chem., Int. Ed. 39*, 250.
46. Tipping, E., Ketterer, B., and Christodoulides, L. (1979) Interactions of small molecules with phospholipid-bilayers—Binding to egg phoshatidylcholine of some organic-anions (bromosulfophthalein, estrone sulfate, heme and bilirubin) that bind to ligandin and aminoazo-dye-binding protein-A. *Biochem. J. 180*, 327–337.
47. Liu, S. C., Zhai, S., Lawler, J., and Palek, J. (1985) Hemin-mediated dissocation of erythrocyte-membrane skeletal proteins. *J. Biol. Chem. 260*, 2234–2239.
48. Cole, C., Barber, J. D., and Barton, G. J. (2008) The Jpred 3 secondary structure prediction server. *Nucleic Acids Res. 36*, W197–W201.